

J. Silva¹, M. Elias², N. Lima³, S. Canevarolo^{1*}

¹Department of Materials Engineering, Federal University of São Carlos, São Paulo, Brazil

²Graduate Program in Materials Science and Engineering, Federal University of São Carlos, São Paulo, Brazil

³Instituto de Pesquisas Energéticas e Nucleares, CCTM, São Paulo, Brazil

Morphology in Multilayer Blown Films of Polypropylene and Ethylene-Octene Copolymer Blends

In this work the microstructure of multilayer blown films consisting of a core layer placed between two external ones is studied. The core layer is a blend with 70% (w/w) of a homopolypropylene PP and 30% of a metallocene-catalyzed ethylene-octene copolymer mEOC (LLDPE or VLDPE), whereas the external symmetrical layers are composed of LLDPE or they have the same composition as the core layer. The PP and PE crystalline phases formed during the film blowing were investigated by thermal analysis, mechanical properties, TEM morphology and X-ray diffraction pole figures. These films successfully combine the high mechanical strength of PP with the quasi-isotropic behavior of blown PE. Multilayer film containing PP/mEOC blends, particularly blends of PP70/LLDPE30, show better balanced tensile properties when compared at crossed directions. The presence of VLDPE in the blends shifts downwards the melting and crystallization temperatures and crystallinity of PP. X-Ray pole figures suggest the occurrence of epitaxial crystallization of the PE phase upon the PP crystals in these PP/mEOC blend films.

1 Introduction

Polyolefins such as polypropylene (PP) and polyethylene (PE) are usually classified as commodities. These materials exhibit a good cost/benefit relation, being broadly used in the flexible packaging industry. A possible route to create films with better properties and/or lower cost than the films of one single material, PP or PE, consists in combining both materials: PE, which is ductile at low temperatures, and PP that has a relatively high tensile strength. However, the poor compatibility between PP and PE and the low interfacial adhesion, resulting from the low surface free energy and lack of polar functional groups

(Awaja et al., 2009), has hindered the commercial success of PP/PE films.

Ethylene-propylene rubber (EPR) (Jancar et al., 1993; Moore, 1996; Nitta et al., 2005; Poelt et al., 2000), copolymer of ethylene-propylene-diene monomer (EPDM) (Bertin and Robin, 2002; Bhadane et al., 2006; Souza and Demarquette, 2002) and ethylene-vinyl acetate copolymer (EVA) (Huerta-Martinez et al., 2005; McEvoy and Krause, 1996) have been used to improve the compatibility and adhesion of PP/PE systems. Alternatively, in recent years, there has been increasing use of metallocene-catalyzed ethylene- α -olefin copolymers (mEC) to improve the melt and impact strength of PP (Chaffin et al., 2000a; b; Da Silva et al., 2002; McNally et al., 2002; Mohanty and Nayak, 2007; Premphet and Paecharoenchai, 2002; Rabinovitch et al., 2003; Yan et al., 2007). It seems that the more uniform branching and narrower molecular weight distributions obtained by the use of single-site catalysts can promote the adhesion and compatibility in PP/PE systems. In fact, although some authors have reported thermodynamical immiscibility between PP and mECs, most of the studies show enhanced interfacial adhesion and compatibility in these polymeric systems (Chaffin et al., 2000a; b; Kukaleva et al., 2000a; b). Rana et al. (1998) studied blends of PP and metallocene-catalyzed ethylene-octene copolymer (mEOC). Notwithstanding the significant shift of PP crystallization peak toward low temperatures as the concentration of mEOC increases, the authors showed that PP and mEOC are thermodynamically immiscible. Nevertheless, their work revealed the mechanical compatibility in the blends. McNally et al. (2002) observed partial miscibility of PP and mEOC provided that the concentration of the latter is low, i. e., 10 wt% or less. Moreover, they reported no alteration in PP crystallization peak maxima but a slight broadening which was attributed to the disruption of the PP crystal morphology by the mEOC. On the other hand, a pronounced increase of the PP crystallization temperature with increasing mEOC concentration (up to 30 wt%) was observed by Kukaleva et al. (2000a; b). The result was explained as being likely due to the increase of interfacial area that acts as a nucleating agent. The authors (Kukaleva et al., 2000a b) concluded that the studied PP/mEOC system is miscible at processing temperatures but immiscible in the solid state. Blends of PP

* Mail address: Sebastião Canevarolo, DEMa – UFSCar, Department of Materials Engineering, Federal University of São Carlos, São Paulo 13565-905, Brazil
E-mail: caneva@ufscar.br

with metallocene-catalyzed ethylene- α -butene (mEBC) and ethylene- α -octene (mEOC) copolymers, prepared by Kontopoulou et al. (2003), have shown to be immiscible but have excellent mechanical compatibility. Additionally, these authors observed no alteration of the PP melting temperature and a decrease of PP crystallization content, indicating that PP phase is prevented to crystallize in the blends in the presence of mECs. Similar conclusion was reached by Wang et al. (2014); they have reported that ethylene-octene copolymer particles act as an obstacle during the crystallization of PP, increasing the grow path of PP lamellae and reducing the grow space of spherulites, thus resulting in a slower spherulite growth rate and smaller spherulite size. Shanks et al. (2000a) compared PP/EC blends containing ECs obtained with Ziegler-Natta catalysts (ZN-EC) with PP/mECs blends. They observed that only mEC was miscible with PP in the melt state, with co-crystallization occurring in this blend. Additionally, it has been shown that the good mechanical compatibility of PP/mEC blends is associated to a lowering of interfacial tension and therefore to a droplet size decrease (Carriere and Silvis, 1997; Kontopoulou et al., 2003; Svoboda et al., 2009a; b).

Chaffin et al. (2000a; b) compared blends of PP and two different ethylene-hexene copolymers (EHC), prepared with Ziegler-Natta and metallocene catalysts. The interfacial failure was predominant in PP/ZN-EHC, which was due to the segregation of low molecular weight amorphous material at the interface. Conversely, in the blends with mEHC, as a result of an efficient crystallite anchoring of interfacially entangled chains, the failure occurred in the PP matrix. The good adhesion between PP and mECs with short-chain branches (SCB) has been reported by other authors. The adhesion of EOCs to PP was studied by Poon et al. (2004a; b). The poorest adhesion was observed for a ZN-EOC with density of $0.925 \text{ g} \cdot \text{cm}^{-3}$ whereas the best adhesions were obtained for mEOC's with higher molecular weights and lower densities ($0.90 \text{ g} \cdot \text{cm}^{-3}$ or less).

The structure of tubular blown films processed from blends of PP/EPR (hmsPP) and two EOC resins (a pure ZN-EOC and a blend ZN-EOC/mEOC) was investigated by Chang et al. (2002a; b; c). They reported that hmsPP increases the tensile modulus and strength without significantly affecting the ultimate elongation. It was argued that the epitaxial crystallization of PE on substrates of oriented PP promoted a strong adhesion and synergy that improved the mechanical properties.

The tear behavior of multilayered sheets, consisting of alternating PP and EOC layers, has also been investigated. He et al. (2016) observed, for a PP/EOC multilayer film, that both the tear strength and energy are higher than those of the corresponding conventional blend.

Despite there are several works in the literature concerning the properties of PP/EOC blends, the studies dealing with the microstructure of PP/EOC blown films are scarce. Moreover, it is known that the blown polymeric films are usually subjected to large strains during cooling and can be highly anisotropic. In this work, multilayer tubular blown films, in which the core layer is a blend of PP/mEOC, are investigated.

2 Experimental

2.1 Materials

In this study, an isotactic homopolypropylene (PP) (density 0.905 g/cm^3 and MFI = 0.80 g/10 min) produced with Ziegler-Natta catalyst by Braskem, Triunfo, Brazil, and two commercial ethylene-octene copolymers manufactured by Dow Chemical Company Bahia Blanca, Argentina, were used. These two mEOC's are a linear low density polyethylene (LLDPE) (density 0.916 g/cm^3) and a linear very-low density polyethylene (VLDPE) (density 0.902 g/cm^3), both with octene comonomer and produced by metallocene process. Some properties of the materials are shown in Table 1.

2.2 Blown Film Preparation

Films with $50 \mu\text{m}$ total thickness were coextruded in a 3-layers industrial type machine (model Vorex, Windmoeller & Hoelscher, Lengerich, Germany) at Itap Bemis Ltda Company (Londrina, PR, Brazil). The extrusion blowing parameters used were a blow-up ratio (BUR) of 1.75, a drawn down ratio (DDR) of 20 and a flow rate of 260 kg/h (the die diameter was 400 mm and the gap used was 1.8 mm). The processing temperature of the extruder delivering the external layers was kept constant at 190°C whereas the temperature in the extruder delivering the core layer was 210°C . The die temperature was kept at 210°C . To make monolayer films both extruders are fed with the same material. The crystallization of multilayer film during

Material	Density g/cm^3	MFI (190°C ; 2,16 kg) g/10 min	Comonomer weight %	Comonomer molar weight %	M_w	M_n	PD
PP	0.905	0.80	0	0	NA	NA	NA
LLDPE	0.916	1.00	15	4.2	110,000	30,000	3.7
VLDPE	0.904	1.00	20	5.9	95,000	35,000	2.7

NA = not available

Table 1. Some physico-chemical properties of pristine ZN homopolypropylene (PP), and metallocene ethylene-octene copolymers (LLDPE and VLDPE)

the processing leads to the formation of two distinct frost lines at about 50 cm and 80 cm height.

The coextruded blown films are composed of three layers with an A/B/A symmetrical structure to avoid warping. Each external layer has a thickness of 12 μm , whereas the core layer is 26 μm thick, producing films with 50 μm final thickness, measured by polarized light optical microscopy of film's cross sections. The first set of films used in this study has all the three layers composed of the same material (either PP, PE or blends of PP/PE); these will be named monolayer films. The second set of films used here are formed from two external layers of LLDPE that ensure the melt seal and a core layer with the blend PP70/LLDPE30 or PP70/VLDPE30, both with a fixed mEOC content of 30% w/w, which imparts a well-balanced mechanical strength to the blow stretched blended film, in comparison to the anisotropic behavior shown by pure PP. This feature will be better discussed along the text.

2.3 Films Characterization

2.3.1 Differential Scanning Calorimetry (DSC)

The melting and crystallization were studied in a DSC calorimeter (model Q200, TA Instruments, New Castle, DE, USA). Heating and cooling rates of 10 $^{\circ}\text{C}/\text{min}$ were used. The crystallinity degree (α_c) of a particular component/phase was obtained calculating the ratio of the measured area (i. e. its enthalpy) under its corresponding melting peak divided by the theoretical values for the melting enthalpy $\Delta H_0^{\text{PP}} = 165\text{J/g}$ (Bu et al., 1988) and $\Delta H_0^{\text{PE}} = 293.6\text{J/g}$ (Wunderlich, 2005), normalized by the component's weight fraction present in the sample (whole film):

$$\alpha_c(\%) = w_i * \frac{\Delta H_{\text{peak}}}{\Delta H_0} * 100\%. \quad (1)$$

When multiple peaks of the same component are present (as in the case of PE) the total peak area was taken and so the total crystallinity degree calculated.

2.3.2 Tensile Strength

The tensile strength tests were performed at room temperature (model 3365, Instron, Canton, USA) following the American Standard ASTM D882-02. The deformation speed was 500 mm/min with an initial distance between the jaws of 50 mm. The samples were cut in MD and TD with dimensions of 25.4 mm (width) and 254 mm (length) and, at least 5 samples were tested. The stress/strain curves were stacked; the one that better represents them all was selected. The shape of the curves was very constant, showing good data reproducibility.

2.3.3 Transmission Electron Microscopy (TEM)

Transmission electron micrographs were obtained by first imbedding each polyolefin film in an epoxy resin, followed by a curing step at room temperature for more than 24 h. The speci-

mens were then microtomed, at -80°C with a diamond knife, in slices with thickness in the range 70 to 80 nm. Then, the samples were stained with RuO₄ vapor for 6 h and viewed in a transmission electron microscope, model CM120, Philips, Eindhoven, The Netherlands.

2.3.4 X-Ray Diffraction (XRD)

Crystallographic texture of polymeric films was evaluated by X-ray diffraction technique using a horizontal texture goniometer (Rigaku, Tokyo, Japan). Measurements were carried out with Cu K α 1 ($\lambda = 0.15405\text{ nm}$) radiation using the back reflection technique as described by Schulz (1949). Three incomplete pole figures ($5^{\circ} \leq \alpha \leq 70^{\circ}$) were measured for each diffraction plane: [1, 1, 0], [2, 0, 0] and [0, 2, 0] for PE (diffraction angle $2\theta = 21.79^{\circ}$, 24.10° , 36.40° respectively) and [1, 1, 0], [0, 4, 0] and [1, 3, 0] for PP (diffraction angle $2\theta = 14.38^{\circ}$, 17.16° , 18.80° respectively).

3 Results and Discussion

3.1 Thermal Analyses

The DSC thermograms of first heating, cooling and second heating are shown in Fig. 1. During the heating of monolayer film of PP a narrow single peak, corresponding to the melting of the lamellar crystals, is observed at 165 $^{\circ}\text{C}$, whereas the monolayer film of LLDPE shows a complex morphology with three peaks: a lower one, broad and centered at 100 $^{\circ}\text{C}$, a middle one sharp and centered at 119 $^{\circ}\text{C}$ and a higher one also sharp and centered at 122 $^{\circ}\text{C}$ (Fig. 1A). The lower and the higher melting peaks are characteristics of the LLDPE, denoting two crystal populations, still present during the second heat. The peak at 119 $^{\circ}\text{C}$ is due to the melting of a fibrillar morphology produced at the external layers, which is absent during the second heat. For VLDPE just one broad endothermic peak, with the maximum slightly below 100 $^{\circ}\text{C}$, is seen during both first and second heating (Fig. 1B). This same set of melting peaks are seen when the PE is blended with the PP matrix forming the PP70/LLDPE30 and PP70/VLDPE30 monolayer film (Fig. 1C and D). The crystallization of LLDPE during cooling extends over a broad range of temperatures (Fig. 1G and H), whereas the exothermic peak corresponding to the crystallization of VLDPE is narrow.

The analysis of the thermal behavior of the PE in the PP70/LLDPE30 and PP70/VLDPE30 multilayer films (Fig. 1E and F) is not straightforward and needs to be done comparatively with all other curves. In fact, the thermal behavior of the polyethylene in the core and external layers are not necessarily equal. At this point is well worth remember that the components of the monolayer films differ from the multilayer ones at the external layer, which in the latter is made of pristine LLDPE. This implies that multilayer films of PP70/VLDPE30 have different polyethylenes in each layer, and on the contrary, all other films have the same polyethylene in both layers.

In Fig. 1, the thermal behavior of PP phase in the blown films can also be observed. For the PP70/LLDPE30 multilayer

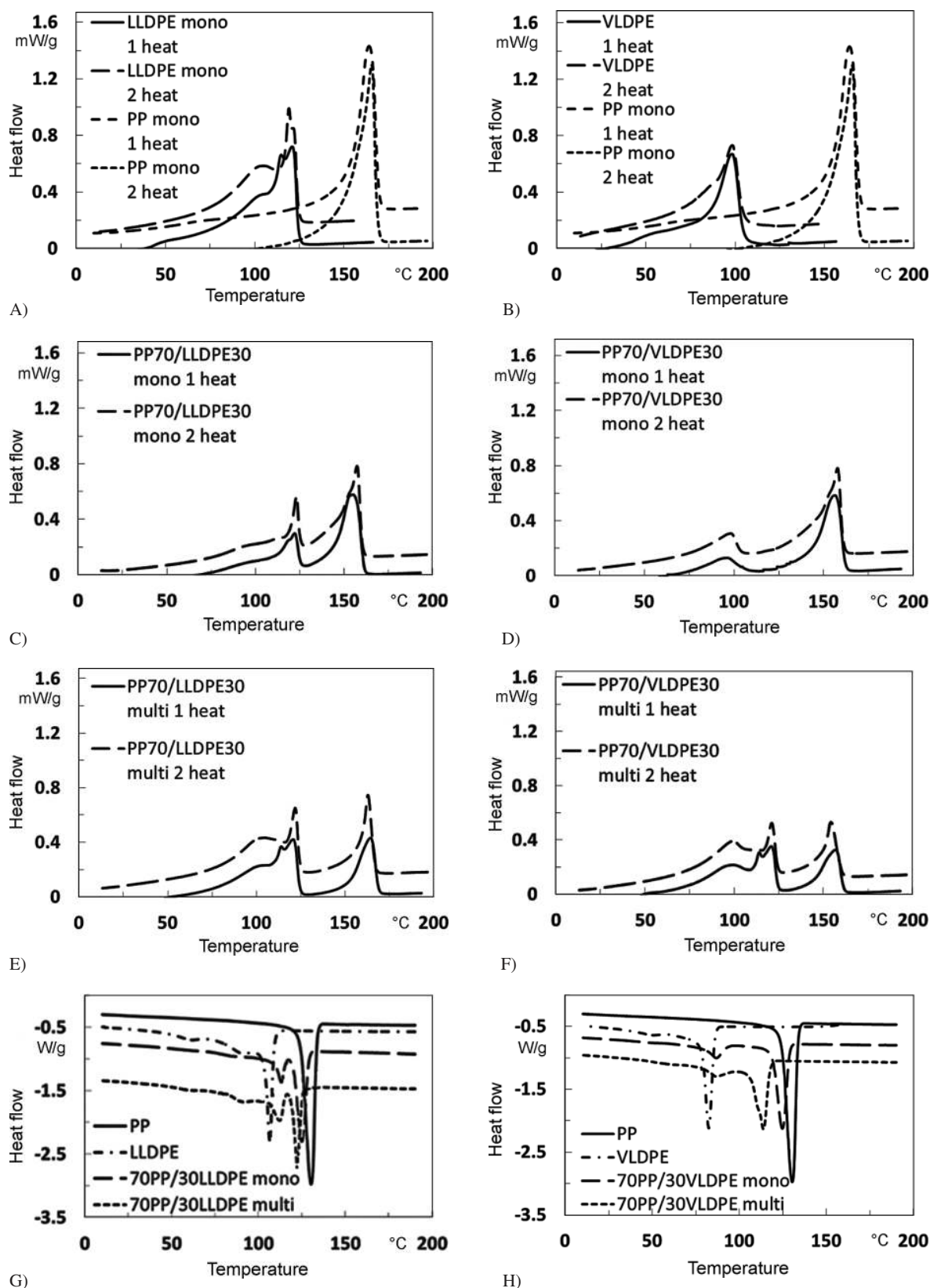


Fig. 1. DSC thermograms with first and second heat cycles of pristine, A) PP and LLDPE, B) PP and VLDPE, C) monolayer films for blends of PP70/LLDPE30, D) PP70/VLDPE30, E) multilayer films of PP70/LLDPE30, F) PP70/VLDPE30; G) and H) DSC crystallization curves of all films used in this study, as indicated

film (Fig. 1E), during heating the PP melting peak (164 °C) is only very slightly shifted downwards relatively to the PP monolayer one (165 °C), whereas during cooling the crystallization temperature of PP decreases about 10 °C. In PP70/VLDPE30 multilayer film (Fig. 1F) a displacement of PP melting and crystallization peaks to lower temperatures is more intense. Moreover, the depression of crystallization temperature of PP, which has also been reported by other authors (Rana et al., 1998; Shanks et al., 2000b), is higher for PP70/VLDPE30 multi (Fig. 1H), reaching almost 20 °C.

The explanation for these observations lies on the blend's morphology. As a matter of fact, it is well-known that crystalline thickness, and in lower extent the degree of crystalline perfection and the crystal lateral dimensions affect the non-equilibrium melting temperature measured in DSC. Thus, the depression of PP melting temperature should be, at least in part, the result of a decrease in the size of the lamellae relatively to those ones formed in pure PP. The presence of the polyethylene in the blends causes not only a decrease in the melting temperature of PP, but also a reduction of its crystalline phase content, as can be seen in the data of Table 2. In general, the chemical potential of a polymer decreases by the addition of a miscible diluent. If the polymer is crystallizable, that decrease in chemical potential will result in a decrease of the

equilibrium melting point, which will be greater the lower is the polymer/polymer interaction parameter, χ (Nishi and Wang, 1975; Rim and Runt, 1984). However, to measure the equilibrium melting points is difficult. The most common way to do it is to follow the method of Hoffmann and Weeks, but even here phase separation will set during the melting and isothermal crystallization cycles, relaxing the unstable original blend morphology, changing it irreversibly.

The results discussed above confirm the difficulty in getting a general pattern for the influence of a mEOC on the PP melting temperature. It should depend upon structural characteristics of the EOC like its specific molecular architecture in terms of the type, concentration and distribution of the comonomer along the copolymer chain, molecular weight and molecular weight distribution. It also should depend upon the mixing process variables like shear level in the die, orientation, blow-up ratio, extrusion/die temperature, etc.

3.2 Morphology

The morphology of the blown blend films was examined by TEM using RuO4 staining technique to highlight the contrast between the two phases. This procedure stains preferably

Film structures		Content %w/w		1° Heating				2° Heating	
		PP	PE	PE		PP		PE	PP
				α_c %	T_m °C	α_c %	T_m °C		
Pristine	PP	100	–	–	–	61	165	–	62
	LLDPE	–	100	42	100; 119; 122	–	–	44	–
	VLDPE	–	100	32	100	–	–	30	–
Monolayer	PP70/LLDPE30	70	30	35	–; 119; 122	46	157	28	46
	PP70/VLDPE30	70	30	20	100	45	157	27	50
Multilayer*	PP70/LLDPE30	36	64	33	100; 119; 122	42	163	33	51
	PP70/VLDPE30	36	64	33	100**	47	157	33	49

* external layers of multilayer films are always made of pristine LLDPE

** the other two melting peaks at 119 °C and 122 °C, seen in the DSC curve, are due to the pristine LLDPE present in the external layer

Table 2. Components weight content (%w/w), degree of crystallinity α_c (%), and peak melting temperatures of PP and PE phases as shown by DSC curves in pristine and blends of monolayer and multilayer film structures

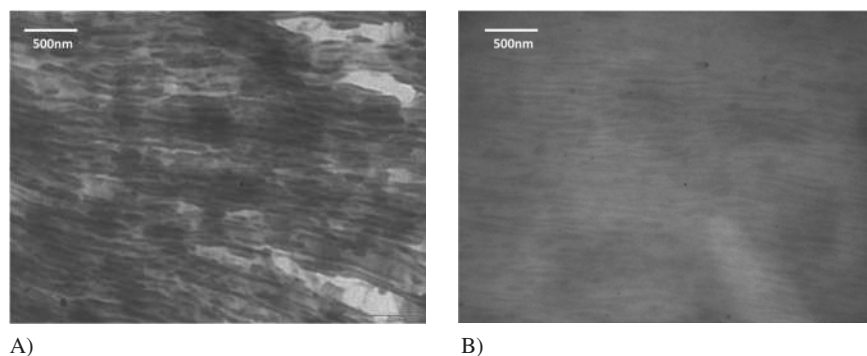


Fig. 2. TEM micrographs of the central layer, A) PP70/LLDPE30, B) PP70/VLDPE30 in multilayer films (same magnification)

EOC (Brown and Butler, 1997; Qureshi et al., 2001), so the darker phase in Fig. 2 can be assigned to this component. Both blends exhibit a lamellar structure with two distinct phases. The more obvious difference between the two blown films, as analyzed by TEM, is the existence of relatively big domains of PP (white areas in Fig. 2A) in some regions of PP/LLDPE, which were not observed for PP/VLDPE. This leaves open the possibility of the existence of thicker lamellae of PP in the PP/LLDPE film, which is consistent with the DSC results. Due to the higher miscibility of the pair PP70/VLDPE30, the crystallization of its PP phase is partially inhibited. The reasons for the higher miscibility of the pair PP/VLDPE should rely on the octene content in the copolymer as well as its molecular architecture. A higher concentration of octene comonomer in VLDPE can contribute to its higher miscibility with PP. The distinct molecular architectures of LLDPE and VLDPE, which can be highly tuned with the metallocene catalysts technology, should also play a decisive role on the different miscibility of the multilayer films. As the details of molecular architectures are not known the mechanical properties of the multilayer films were investigated.

3.3 Mechanical Behavior and Crystallographic Texture

The tensile stress-strain curves of the films are shown in Fig. 3. Here, the imbalance in the mechanical properties of PP monolayer film is also observed (Fig. 3A). When it is stretched in TD, the PP monolayer film suffers brittle rupture, whereas in MD the film is ductile. This behavior indicates an imbalanced-oriented crystalline structure, which, in fact, was confirmed by the X-ray diffraction results shown in Fig. 4. The pole figures of the PP monolayer film (Fig. 4A) show two texture components, which for clarity are labeled I and II. The orientation component I is more intense and it corresponds to c-axis [001] aligned with MD with the b [010] and a [100] axes rotating around it. Thus, the component I should consist of shish-kebab structures aligned with MD. The component II indicates the presence of lamellae with the c and b-axes aligned with TD and ND, respectively. Therefore, the highly anisotropic mechanical behavior of PP monolayer film is explained by the existence of shish-kebabs oriented with MD but not with TD.

Contrariwise, the behavior of LLDPE film is relatively isotropic under tensile load (Fig. 3A). Again, the crystalline structure was investigated by X-ray diffraction (Fig. 5A). The component I, which appears more well-defined than the component II, indicates the a'-axis [110] oriented toward MD, but inclined roughly 20° out of the plane of the film. Therefore, this fits into the Keller/Machin I morphology (a-texture) (Brown and Butler, 1997), which has been usually observed in LLDPE (Lu et al., 2001; Lu and Sue, 2001) and LDPE (Desper, 1969; Pazur and Prudhomme, 1996) blown films. According to this picture, the lamellae grow laterally outward in the form of twisted ribbons with the growth direction parallel to the b-axis and a preferential orientation of the a-axis toward MD.

The blend PP70/LLDPE30 multilayer film exhibits a quasi-isotropic behavior with good mechanical properties (Fig. 3B): the yield strength and tensile strength are about twice as much as for LLDPE monolayer film (Fig. 3A). In fact, the yield strength has an additive correlation but the stress and elonga-

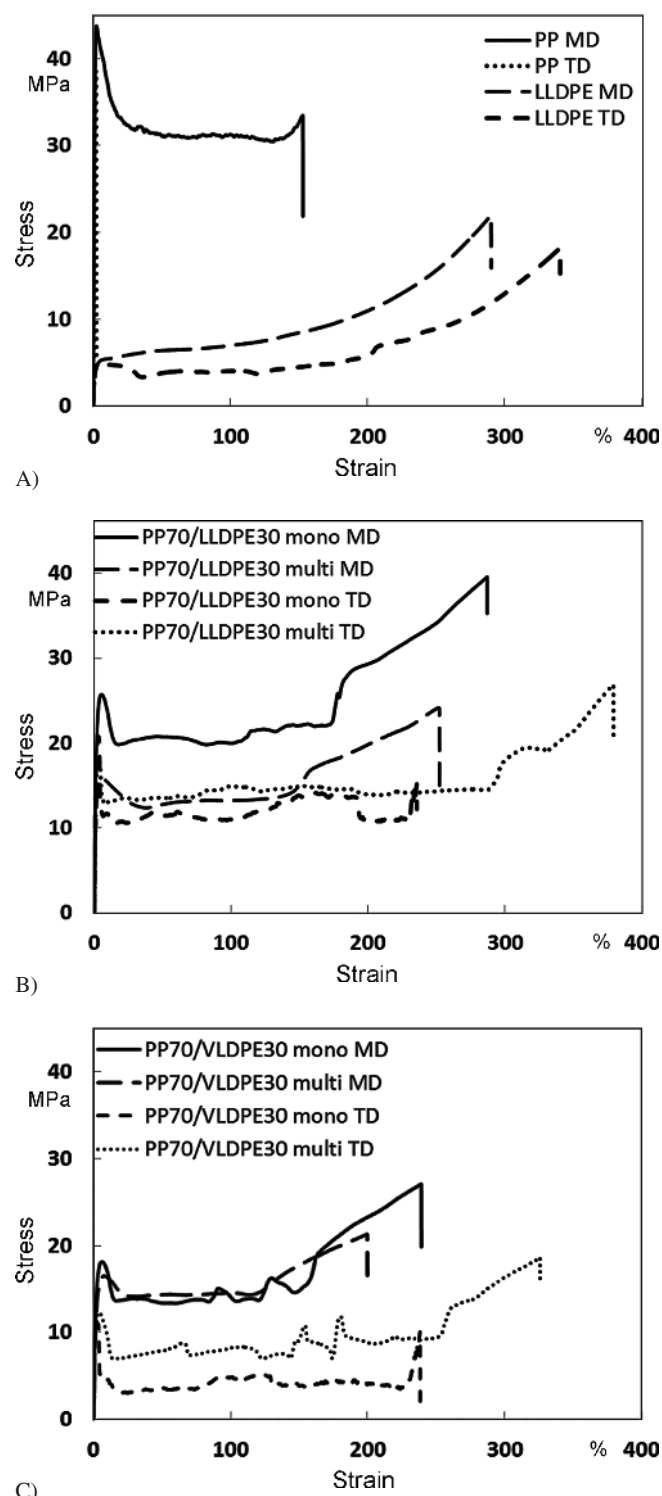


Fig. 3. Tensile stress-strain curves for mono and multilayer films, A) PP and LLDPE monolayer films in machine (MD) and transversal (TD) directions, as indicated. Note the very low elongation at rupture for PP monolayer in TD (< 2%) and the low mechanical strength of the LLDPE. B) blends of PP70/LLDPE30 mono and multilayer films in MD and TD directions and C) Blends of PP70/VLDPE30 mono and multilayer films in MD and TD directions, as indicated

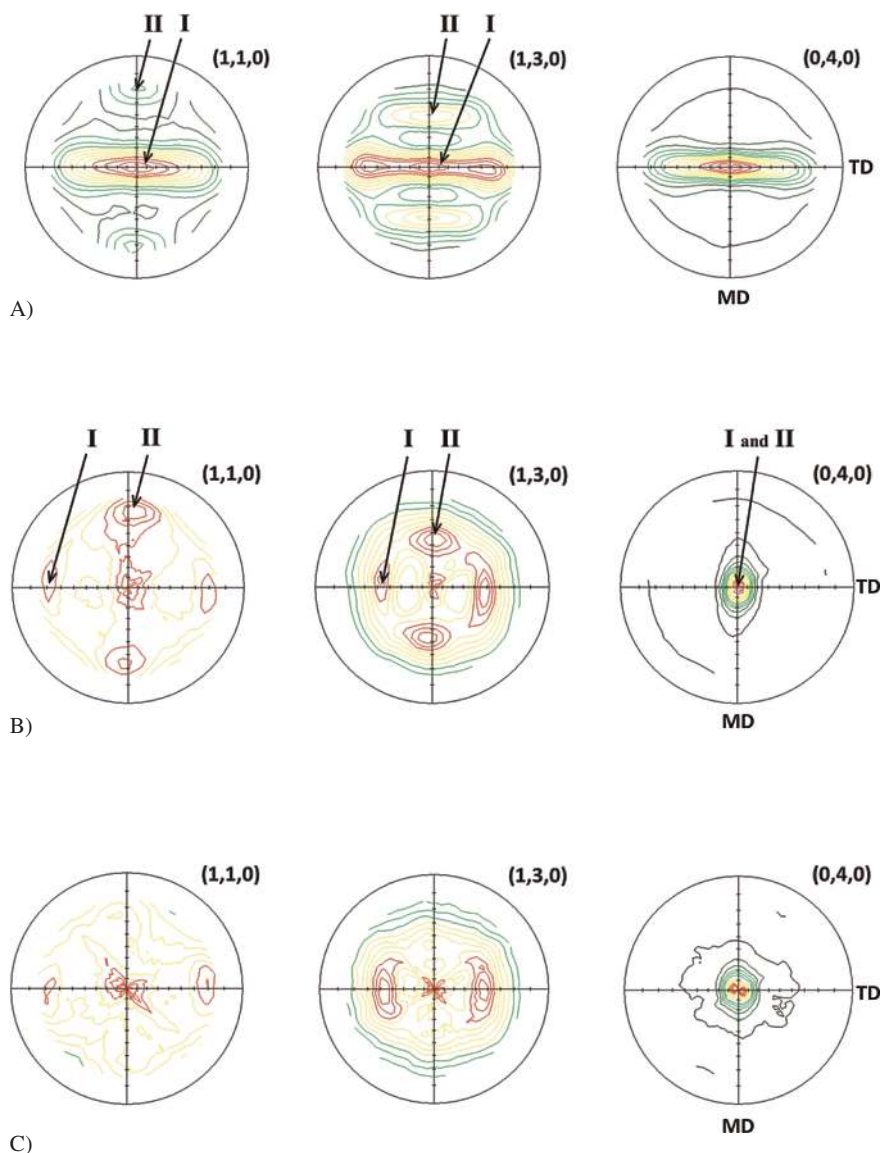


Fig. 4. X-ray pole figures of the (110), (130), (040) planes of the monoclinic crystals of polypropylene PP in monolayer films. A) PP, B) blends of PP70/LLDPE30, C) blends of PP70/VLDPE30 films

tion at rupture overcome the values predicted by an additive behavior. On the other hand, blends with VLDPE (Fig. 3C) show a very anisotropic mechanical behavior.

In order to relate the mechanical results of multilayer films with the orientation of the crystalline phases in its core layers, pole figures were obtained for PP70/LLDPE30 monolayer and PP70/VLDPE30 monolayer films, in which the external layers are composed of the same blend as one of the core. The crystalline orientation of PP crystals is presented in Fig. 4 and the polyethylene crystals in Fig. 5. A first inspection of the pole figures of the PP phase of the PP70/LLDPE30 and PP70/VLDPE30 monolayer films (Fig. 4B and C) reveals that the shish-kebab structures are not present anymore. Instead, on both films the crystalline phase of PP seems to consist almost exclusively of lamellae. In the PP70/LLDPE30 monolayer film there are two groups of lamellae with approximately the same size and well-defined orientations (Fig. 4B): the component I has the c-axis in the MD and the b-axis in ND, whereas in the component II the c-axis is aligned in TD. Moreover, the pole

figures corresponding to the PE phase of PP70/LLDPE30 monolayer film (Fig. 5B) indicate the existence of a well-defined main orientation component I with the a-axis pointing in ND and the b-axis laying in TD-MD plane and doing an angle of about 40 to 50° with MD. This texture is a strong indication that PP lamellae form row nucleated structures upon which the lamellae of polyethylene crystallizes epitaxially. The enhancement of the ultimate elongation and strength of the PP70/LLDPE30 film relatively to LLDPE, seen in Fig. 3B, is probably due to epitaxial crystallization. Besides, the well balanced crystalline texture should explain the quasi-isotropic mechanical behavior of the PP70/LLDPE30 multilayer films.

Contrarily, the mechanical behavior of the PP70/VLDPE30 multilayer film during the tensile stress-strain test (Fig. 3C) does show a great anisotropy. It's rupture occurs at lower elongations, which can be related with the lower degree of crystallinity of the polyethylene phase, approx. 20%, compared to approx. 35% for PP70/LLDPE30 (see Table 2).

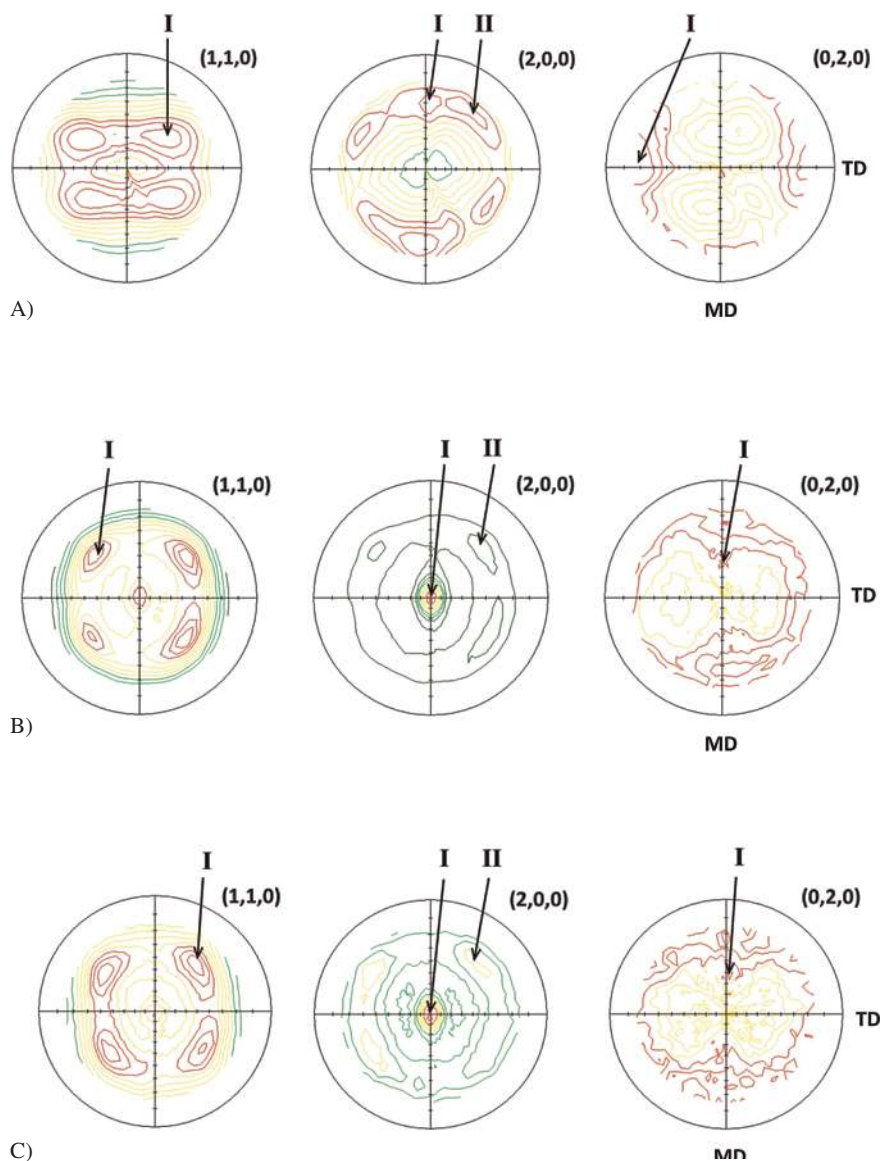


Fig. 5. X-ray pole figures of the (110), (200), (020) planes of the orthorhombic crystals of polyethylene PE in monolayer films, A) pristine LLDPE, B) blends of PP70/LLDPE30, C) blends of PP70/VLDPE30

The pole figures of the crystalline PP phase of PP70/VLDPE30 monolayer films (Fig. 4C) show a clear orientation of the c-axis of the PP unitary cell around MD only. The component II is absent or at least its fraction is much lower than that of component I. Nevertheless, both monolayer films, PP70/LLDPE30 and PP70/VLDPE30, have equal PP melting temperatures and degree of crystallinity, as measured by DSC (Table 2). Just as observed previously, the pole figures corresponding to the PE phase (Fig. 5C) of PP70/VLDPE30 monolayer films also indicate epitaxial crystallization.

4 Conclusions

A polypropylene PP and two metallocene-catalyzed ethylene-octene copolymers mEOC (LLDPE and VLDPE) were used to manufacture multilayer blown films. These films combine the quasi-isotropy of polyethylene, especially regarding to stress and elongation at rupture, with the higher mechanical strength

of polypropylene. Pure PP oriented films have highly anisotropic mechanical behavior due to the presence of shish-kebabs oriented with MD. Multilayer film containing PP/mEOC blends, particularly blends of PP70/LLDPE30, show better balanced tensile properties when compared at crossed directions. The presence of VLDPE in the blends shifts downwards the melting and crystallization temperatures and crystallinity of PP. X-Ray pole figures indicate epitaxial crystallization of the PE phase upon the PP crystals in these PP/mEOC blends.

References

- Awaja, F., Gilbert, M., Kelly, G., Fox, B. and Pigram, P. J., "Adhesion of Polymers", *Prog. Polym. Sci.*, **34**, 948–968 (2009), DOI:10.1016/j.progpolymsci.2009.04.007
- Bertin, S., Robin, J. J., "Study and Characterization of Virgin and Recycled LDPE/PP Blends", *Eur. Polym. J.*, **38**, 2255–2264 (2002), DOI:10.1016/S0014-3057(02)00111-8

- Bhadane, P. A., Champagne, M. F., Huneault, M. A., Tofan, F. and Favis, B. D., "Continuity Development in Polymer Blends of Very Low Interfacial Tension", *Polymer*, **47**, 2760–2771 (2006), DOI:10.1016/j.polymer.2006.01.065
- Brown, G. M., Butler, J. H., "New Method for the Characterization of Domain Morphology of Polymer Blends Using Ruthenium Tetroxide Staining and Low Voltage Scanning Electron Microscopy (LVSEM)", *Polymer*, **38**, 3937–3945 (1997), DOI:10.1016/S0032-3861(96)00962-7
- Bu, H. S., Cheng, S. Z. D. and Wunderlich, B., "Addendum to the Thermal-Properties of Polypropylene", *Makromol. Chem. Rapid*, **9**, 75–77 (1988), DOI:10.1002/marc.1988.030090205
- Carriere, C. J., Silvis, H. C., "The Effects of Short-Chain Branching and Comonomer Type on the Interfacial Tension of Polypropylene-Polyolefin Elastomer Blends", *J. Appl. Polym. Sci.*, **66**, 1175–1181 (1997), DOI:10.1002/(SICI)1097-4628(19971107)66:6<1175::AID-APP17>3.0.CO;2-0
- Chaffin, K. A., Bates, F. S., Brant, P. and Brown, G. M., "Semicrystalline Blends of Polyethylene and Isotactic Polypropylene: Improving Mechanical Performance by Enhancing the Interfacial Structure", *J. Polym. Sci., Part B: Polym. Phys.*, **38**, 108–121 (2000a), DOI:10.1002/(SICI)1099-0488(20000101)38:1<108::AID-POLB14>3.0.CO;2-9
- Chaffin, K. A., Knutsen, J. S., Brant, P. and Bates, F. S., "High-Strength Welds in Metalocene Polypropylene/Polyethylene Laminates", *Science*, **288**, 2187–2190 (2000b), PMID:10864863; DOI:10.1126/science.288.5474.2187
- Chang, A. C., Chum, S. P., Hiltner, A. and Baer, E., "Mechanisms of Ductile Tear in Blown Film from Blends of Polyethylene and High Melt Strength Polypropylene", *Polymer*, **43**, 6515–6526 (2002a), DOI:10.1016/S0032-3861(02)00304-X
- Chang, A. C., Inge, T., Tau, L., Hiltner, A. and Baer, E., "Tear Strength of Ductile Polyolefin Films", *Polym. Eng. Sci.*, **42**, 2202–2212 (2002b), DOI:10.1002/pen.11110
- Chang, A. C., Tau, L., Hiltner, A. and Baer, E., "Structure of Blown Film from Blends of Polyethylene and High Melt Strength Polypropylene", *Polymer*, **43**, 4923–4933 (2002c), DOI:10.1016/S0032-3861(02)00304-X
- Da Silva, A. L. N., Rocha, M. C. G., Coutinho, F. M. B., Bretas, R. E. S. and Farah, M., "Evaluation of Rheological and Mechanical Behavior of Blends Based on Polypropylene and Metalocene Elastomers", *Polym. Test.*, **21**, 647–652 (2002), DOI:10.1016/S0142-9418(01)00084-8
- Desper, C. R., "Structure and Properties of Extruded Polyethylene Film", *J. Appl. Polym. Sci.*, **13**, 169–191 (1969), DOI:10.1002/app.1969.070130117
- He, G. S., Zhang, F. S., Yu, H. N., Li, J. and Guo, S. Y., "Ductile Tear Behavior of Multilayered Polypropylene Homopolymer/Ethylene 1-Octene Copolymer Sheets", *J. Appl. Polym. Sci.*, **133**, 43298 (2016), DOI:10.1002/app.43298
- Huerta-Martinez, B. M., Ramirez-Vargas, E., Medellin-Rodriguez, F. J. and Garcia, R. C., "Compatibility Mechanisms between EVA and Complex Impact Heterophase PP-EPx Copolymers as a Function of EP Content", *Eur. Polym. J.*, **41**, 519–525 (2005), DOI:10.1016/j.eurpolymj.2004.10.021
- Jancar, J., Dianselmo, A., Dibenedetto, A. T. and Kucera, J., "Failure Mechanics in Elastomer Toughened Polypropylene", *Polymer*, **34**, 1684–1694 (1993), DOI:10.1016/0032-3861(93)90328-8
- Kontopoulou, M., Wang, W., Gopakumar, T. G. and Cheung, C., "Effect of Composition and Comonomer Type on the Rheology, Morphology and Properties of Ethylene-Alpha-Olefin Copolymer/Polypropylene Blends", *Polymer*, **44**, 7495–7504 (2003), DOI:10.1016/j.polymer.2003.08.043
- Kukuleva, N., Cser, F., Jollands, M. and Kosior, E., "Comparison of Structure and Properties of Conventional and 'High-Crystallinity' Isotactic Polypropylenes and Their Blends with Metalocene-Catalyzed Linear Low-Density Polyethylene. I. Relationships between Rheological Behavior and Thermal and Physical Properties", *J. Appl. Polym. Sci.*, **77**, 1591–1599 (2000a), DOI:10.1002/1097-4628(20000815)77:7<1591::AID-APP20>3.0.CO;2-M
- Kukuleva, N., Jollands, M., Cser, F. and Kosior, E., "Influence of Phase Structure on Impact Toughening of Isotactic Polypropylene by Metalocene-Catalyzed Linear Low-Density Polyethylene", *J. Appl. Polym. Sci.*, **76**, 1011–1018 (2000b), DOI:10.1002/(SICI)1097-4628(20000516)76:7<1011::AID-APP4>3.0.CO;2-Q
- Lu, J., Sue, H. J. and Rieker, T. P., "Dual Crystalline Texture in HDPE Blown Films and Its Implication on Mechanical Properties", *Polymer*, **42**, 4635–4646 (2001), DOI:10.1016/S0032-3861(00)00719-9
- Lu, J. J., Sue, H. J., "Characterization of Crystalline Texture of LLDPE Blown Films Using X-Ray Pole Figures", *Macromolecules*, **34**, 2015–2017 (2001), DOI:10.1021/ma001031h
- Mcevoy, R. L., Krause, S., "Interfacial Interactions between Polyethylene and Polypropylene and Some Ethylene-Containing Copolymers", *Macromolecules*, **29**, 4258–4266 (1996), DOI:10.1021/ma951768k
- McNally, T., Meshane, P., Nally, G. M., Murphy, W. R., Cook, M. and Miller, A., "Rheology, Phase Morphology, Mechanical, Impact and Thermal Properties of Polypropylene/Metalocene Catalysed Ethylene 1-Octene Copolymer Blends", *Polymer*, **43**, 3785–3793 (2002), DOI:10.1016/S0032-3861(02)00170-2
- Mohanty, S., Nayak, S. K., "Dynamic-Mechanical and Thermal Characterization of Polypropylene/Ethylene-Octene Copolymer Blend", *J. Appl. Polym. Sci.*, **104**, 3137–3144 (2007), DOI:10.1002/app.25941
- Nishi, T., Wang, T. T., "Melting-Point Depression and Kinetic Effects of Cooling on Crystallization in Poly(vinylidene fluoride) Poly(methyl methacrylate) Mixtures", *Macromolecules*, **8**, 909–915 (1975), DOI:10.1021/ma60048a040
- Nitta, K. H., Shin, Y. W., Hashiguchi, H., Tanimoto, S. and Terano, M., "Morphology and Mechanical Properties in the Binary Blends of Isotactic Polypropylene and Novel Propylene-Co-Olefin Random Copolymers With Isotactic Propylene Sequence 1. Ethylene-Propylene Copolymers", *Polymer*, **46**, 965–975 (2005), DOI:10.1016/j.polymer.2004.11.033
- Pazur, R. J., Prudhomme, R. E., "X-Ray Pole Figure and Small Angle Scattering Measurements on Tubular Blown Low-Density Poly(ethylene) Films", *Macromolecules*, **29**, 119–128 (1996), DOI:10.1021/ma9464229
- Poelt, P., Ingolic, E., Gahleitner, M., Bernreitner, K. and Geymayer, W., "Characterization of Modified Polypropylene by Scanning Electron Microscopy", *J. Appl. Polym. Sci.*, **78**, 1152–1161 (2000), DOI:10.1002/1097-4628(20001031)78:5<1152::AID-APP250>3.0.CO;2-7
- Poon, B. C., Chum, S. P., Hiltner, A. and Baer, E., "Adhesion of Polyethylene Blends to Polypropylene", *Polymer*, **45**, 893–903 (2004a), DOI:10.1016/j.polymer.2003.11.018
- Poon, B. C., Rogunova, M., Chum, S. P., Hiltner, A. and Baer, E., "Classification of Homogeneous Copolymers of Propylene and 1-Octene Based on Comonomer Content", *J. Polym. Sci., Part B: Polym. Phys.*, **42**, 4357–4370 (2004b), DOI:10.1002/polb.20290
- Premphet, K., Paecharoenchai, W., "Polypropylene/Metalocene Ethylene-Octene Copolymer Blends with a Bimodal Particle Size Distribution: Mechanical Properties and Their Controlling Factors", *J. Appl. Polym. Sci.*, **85**, 2412–2418 (2002), DOI:10.1002/app.10886
- Qureshi, N. Z., Rogunova, M., Stepanov, E. V., Capaccio, G., Hiltner, A. and Baer, E., "Self-Adhesion of Polyethylene in the Melt. 2. Comparison of Heterogeneous and Homogeneous Copolymers", *Macromolecules*, **34**, 3007–3017 (2001), DOI:10.1021/ma000583x
- Rabinovitch, E. B., Summers, J. W. and Smith, G., "Impact Modification of Polypropylene", *J. Vinyl. Add. Tech.*, **9**, 90–95 (2003), DOI:10.1002/vnl.10068
- Rana, D., Lee, C. H., Cho, K., Lee, B. H. and Choe, S., "Thermal and Mechanical Properties for Binary Blends of Metalocene Polyethylene with Conventional Polyolefins", *J. Appl. Polym. Sci.*, **69**, 2441–2450 (1998), DOI:10.1002/(SICI)1097-4628(19980919)69:12<2441::AID-APP15>3.0.CO;2-#

- Rim, P. B., Runt, J. P., "Melting-Point Depression in Crystalline Compatible Polymer Blends", *Macromolecules*, **17**, 1520–1526 (1984), DOI:10.1021/ma00138a017
- Schulz, L. G., "Determination of Preferred Orientation in Flat Transmission Samples Using a Geiger Counter X-Ray Spectrometer", *J. Appl. Phys.*, **20**, 1033–1035 (1949), DOI:10.1063/1.1698268
- Shanks, R. A., Li, J., Chen, F. and Amarasinghe, G., "Time-Temperature-Miscibility and Morphology of Polyolefin Blends", *Chinese J. Polym. Sci.*, **18**, 263–270 (2000a)
- Shanks, R. A., Li, J. and Yu, L., "Polypropylene-Polyethylene Blend Morphology Controlled by Time-Temperature-Miscibility", *Polymer*, **41**, 2133–2139 (2000b), DOI:10.1016/S0032-3861(99)00399-7
- Souza, A. M. C., Demarquette, N. R., "Influence of Coalescence and Interfacial Tension on the Morphology of PP/HDPE Compatibilized Blends", *Polymer*, **43**, 3959–3967 (2002), DOI:10.1016/S0032-3861(02)00223-9
- Svoboda, P., Svobodova, D., Slobodian, P., Ougizawa, T. and Inoue, T., "Crystallization Kinetics of Polypropylene/Ethylene-Octene Copolymer Blends", *Polym. Test.*, **28**, 215–222 (2009a), DOI:10.1016/j.polymertesting.2008.12.007
- Svoboda, P., Svobodova, D., Slobodian, P., Ougizawa, T. and Inoue, T., "Transmission Electron Microscopy Study of Phase Morphology in Polypropylene/Ethylene-Octene Copolymer Blends", *Eur. Polym. J.*, **45**, 1485–1492 (2009b), DOI:10.1016/j.eurpolymj.2009.01.032
- Wang, J. F., Guo, J. W., Li, C. H., Yang, S., Wu, H. and Guo, S. Y., "Crystallization Kinetics Behavior, Molecular Interaction, and Impact-Induced Morphological Evolution of Polypropylene/Poly(ethylene-co-octene) Blends: Insight into Toughening Mechanism", *J. Polym. Res.*, **21**, 618 (2014), DOI:10.1007/s10965-014-0618-x
- Wunderlich, B.: *Thermal Analysis of Polymeric Materials*, Springer, Berlin (2005)

- Yan, X. L., Xu, X. H. and Zhu, L., "Analysis of Brittle-Ductile Transition of Polypropylene/Ethylene-Octene Copolymer Blends by Scanning Electron Microscopy and Small Angle Laser Light Scattering", *J. Mater. Sci.*, **42**, 8645–8651 (2007), DOI:10.1007/s10853-007-1882-5

Acknowledgements

The authors would like to acknowledge Itap Bemis Ltda and Motechfilm for the preparation of the PP/PE mono and multi-layer films. This work was possible thanks to the financial support from CAPES through Grant BJT 019/2012 to J. M. J. S. and from CNPq through a PQ 311790/2013-5 scholarship to S. V. C.

Date received: June 19, 2017

Date accepted: January 18, 2018

Bibliography DOI 10.3139/217.3526 Intern. Polymer Processing XXXIII (2018) 3; page 345–354 © Carl Hanser Verlag GmbH & Co. KG ISSN 0930-777X
